Translocation of a stiff polymer in a microchannel

Alexandra ten Bosch, Pierre Cheyssac

Translocation of a stiff polymer in a microchannel

A. ten Bosch* and P. Cheyssac

Laboratoire de Physique de la Matiere Condensee,

CNRS 6622,Parc Valrose,F-06108 Nice Cedex 2, France

(Dated: July 4, 2008)

Abstract

The voltage driven dynamics of a stiff polymer through a nanopore are treated with a bend elastic model. In contrast to flexible polymers described by a stretch elasticity, bend elastic chains can be oriented in an external field, here the anchoring field created by the pore atoms. The trajectory of the chain is calculated using the Langevin equation of motion. The dynamical equation is solved by a normal mode analysis of the elastic curve with free ends. Interaction with the pore walls acts to align the chain, interaction with the electric field induced inside the pore dominates the translocation time. Application of a force proportional to the distance of the exit to the end of the pore such as an optical trap slows down the motion, and reduces the chain response to the wall potential and the extension along the pore axis. DNA is a well-known semi rigid polymer and a comparison is made to the molecular dynamics simulation of translocation of DNA through a synthetic nanopore.

1.INTRODUCTION

Industrial applications based on the flow of dilute solutions of polymers in pores of diameters ranging from nanometers to microns are ubiquitous. Recent work has concentrated on the dynamics and structure of biopolymers, in particular as a tool for the analysis and manipulation of DNA sequences [1, 2]. In order to advance the technology it is essential to characterize the conformations of the macromolecule and the events taking place inside the pore in detail. Dynamics modeling should lead to predictive models of how macromolecules behave in microfluidic flows, useful for device design and optimization. Langevin dynamics is most commonly used and is based on rapid collisions of solvent and pore wall molecules with the diffusing Brownian particle[3–9]. The resulting loss of information with respect to a detailed molecular dynamics simulation [10–12] is offset by a relative ease of calculation. In order to fully describe dynamic phenomena either by analytical calculation or by numerical simulation, multiscale methods have also been proposed and especially interesting is a first principle's calculation of the chemical structure of the single macromolecule to determine the parameters of the simple model used in an analytical method for the dynamics.

The dynamics of a polymer chain span a large range of time and length scales, from picoseconds and Angstrom for the individual molecule segments to hours and cm for domain motion in polymer crystals. For example in the spectrum of vibrations of a polymer on the scale of inter atomic vibrations the series of discrete high frequency lines is characteristic of the motion of the molecular building blocks of the chain. On the macroscopic level of acoustic waves, the details of the individual chain structure are not essential to the collective low frequency modes. A continuum monomer density distribution with reasonable elastic coefficients will suffice to describe the wide spectrum of sound propagation in an elastic material. Of special interest is the range between these two limits. The relaxation of chain deformation superimposed on the drift caused by external sources determines the dynamics in dilute solution. Calculations assume a simple model chain structure with reasonable values of single chain friction, segment length or elastic spring constants. Models that have been used with success are the elastic chain, the bead spring or the bead rod polymer [13]. Unfortunately, only the dynamics of flexible chains are easy to manipulate and only if the

motion of a single chain is decoupled from the surrounding chains. Most macromolecules are semi-rigid and resist bending, many have a helix structure, and this is especially true of the natural and biological polymers such as DNA, many of which even form liquid crystal phases.

The elastic worm like chain has been used successfully to describe equilibrium properties of semi rigid polymers [14–16]. The complex chemical structure of the macromolecule is replaced by an elastic chain of degree of polymerization N (or total arc length L), of stretch elastic coefficient κ and bend elastic coefficient ϵ. The polymer conformation is described by a continuous chain at arc length s from the first monomer and position $\vec{r}\ (s)$ with bend described by the change in tangent vector $\vec{dr}\ (s)/ds$ along the chain as well as stretch described by the change in position vector. Early work already considered the coupling of the tangent vector to the local orientation and the validity of the relation valid for a geometric curve $\left|\frac{d\vec{r}}{ds}\right| = 1$ [17–19]. The problem is still being explored as well as the need to include bend and torsion of polymer chains in dynamic properties [20, 21].

In rigid and semi-rigid systems the long range intermolecular interaction depends on the relative orientation of the particles. In particular in the neighborhood of a surface an anchoring force determines a preference for a fixed direction relative to the surface [13, 22–25]. In nanopores, the range of wall effects can easily extend over the whole pore width. The nature of the force can be steric, chemical with formation of covalent or ionic bonds, or electrostatic with formation of a surface charge or dipolar with induced or permanent dipoles. External forces such an imposed electric field can orient the semi rigid polymer but the effect is small. Coupling to the induced dipoles along the chain backbone leads to an additional orientation dependent term in the bend elasticity. For a charged polyelectrolyte such as DNA the electric field mainly works to pull the polymer through the pore accelerating the otherwise slow random diffusion.

2.THEORY AND RESULTS

2.1 The Langevin equation

The Langevin equation of motion of the polymer is

$$m\frac{\partial^2 \vec{r}\ (s,t)}{\partial t^2} + m\zeta\frac{\partial \vec{r}\ (s,t}{\partial t} + \epsilon\frac{\partial^4 \vec{r}\ (s,t)}{\partial s^4} - \kappa\frac{\partial^2 \vec{r}\ (s,t)}{\partial s^2} - \vec{F} - \vec{A}\ (s,t) = 0 \qquad (1)$$

The monomer mass is m and the first term is the inertia. The second term is the internal friction force. The next terms are the stretch and bend elasticity for the continuous elastic chain. The external force is given by $\vec{F}$=$\vec{F_W}$ + $\vec{F_E}$, here the pore wall interaction $\vec{F}_W$ and the electric field $\vec{F}_E$. The last term on the left is the random force, here white noise $\vec{A}\ (s,t)$.

The interaction between the pore wall atoms and the polymer chain is expanded in spherical harmonics in the orientation of the monomer at position $\vec{r}\ (s)$ [22]. The isotropic interactions will not be considered in the case of a pore width sufficiently large ($\geq$2nm) and pore length sufficiently small to avoid significant overlapping and interaction of monomers during translocation [26]. The main effect of the pore walls is then to orient the monomers parallel to the axis along z of the nanopore [10]. Due to symmetry of the pore entrance and exit and of the head and tail polymer chain, the first orientation dependent term is a function of $(dz/ds)^2$. The model mean field interaction parameter W describes the dominant friction force for a given distribution of pore atoms. For anchoring to occur along the pore axis, roughness (variations along the z axis) of pore walls must be considered. The force in the z-direction is then

$$F_W = \frac{W}{2}(3(\frac{\partial z}{\partial s})^2 - 1) \qquad (2)$$

For orientation parallel to z, the average force must be positive and W$\geq$0.

The membrane with a single pore is placed in the center of the translocation cell. A constant voltage is applied between the two electrodes of the cell. Surface charges are induced on the surface of the dielectric membrane material by the external field E_0, strongly distorting the field at the pore entrance [27, 28]. The model for the electric field, discussed in appendix I, is

$$E(z) = \frac{E_0}{\epsilon_m}(\frac{z}{\sqrt{z^2+R^2}} + \frac{H-z}{\sqrt{(H-z)^2+R^2}} + 1) \quad (3)$$

A uniform charge distribution e on the polymer chain couples to the screened applied electric field; the electrostatic interaction between monomers is also strongly screened by the counter ions in the solvent [29, 30]. Inside the pore, a coupling term $p_z\frac{dE(z)}{dz}$ to the permanent dipoles of the polymer with dipole moment p_z must be included in the total electrostatic force along z. An expansion at the pore center is used and $F_{E,z} = F_0 + F_1 z$ with F_0 the total electric force at the center of the pore at $z = H/2, r = 0$. Experiments have been made in the presence of an optical trap placed at the end of the pore. A field is created proportional to the distance of the chain to the pore end as given by the term in $F_1 \leq 0$.

The parameters of the model are the geometry of the cylindrical pore (radius R and length H), the total length L of the polymer, the monomer size a, the elastic coefficents ϵ and κ, the dipole moment $\vec{p}$ and effective charge e of the polymer; the external electric field E_0 , the dielectric constant ϵ_m and friction constant ζ of the solvent and finally the strength W of the pore wall anchoring force. The interaction parameters are effective parameters which can be fit to a given experimental system and for a given polymer are dependent on the material of the pore, the solvent and concentration of free ions. For example for DNA ϵ/kTa can vary between 50 and 150nm for decreasing salt concentration [4, 31, 32]. The model equation along the pore axis is then

$$m\frac{\partial^2 z(s,t)}{\partial t^2} + m\zeta\frac{z(s,t}{\partial t} + \epsilon\frac{\partial^4 z(s,t)}{\partial s^4} - \kappa\frac{\partial^2\ \vec{r}\ (s,t)}{\partial s^2} - \frac{W}{2}(3(\frac{\partial z}{\partial s})^2 - 1) - F_0 - zF_1 = A(s,t) \quad (4)$$

Perpendicular to the pore axis in the x and y directions, the motion is that of a free chain $F_x = F_y = 0$

The random thermal force for stiff chains satisfies the usual conditions;

$$< A(s,t) >= 0 \quad (5)$$

$$< A(s,t)A(s',t') >= 4kT\zeta\delta(t-t')\delta(s-s') \quad (6)$$

2.2 Solution for the polymer modes

To investigate the dynamics including changes in conformation of the chain, an expansion in the bend eigenfunctions is used [33]:

$$z(s,t) = \sum_{p=0} u_p(s) q_p(t) \tag{7}$$

where $q_p(t) = \int ds z(s,t) u_p(s)/L$. The eigenfunctions $u_p(s)$ are solutions of

$$\epsilon \frac{\partial^4 u_p(s)}{\partial s^4} - \kappa \frac{\partial^2 \vec{r}\ (s,t)}{\partial s^2} = (\epsilon \alpha_p^4 - \kappa \alpha_p^2) u_p(s) \tag{8}$$

and fulfill the boundary conditions for free ends of the polymer chain. The set of eigenfunctions is orthonormal: $\int ds u_p(s) u_{p'}(s)/L = \delta(p,p')$.

2.2.1. Case $p > 0$:

The eigenvalues are α_p and the eigenfunctions for p > 0 are

$$u_p = c_0 \exp(\alpha_p s) + c_1 \exp(i\alpha_p s) + c_2 \exp(-\alpha_p s) + c_1^* \exp(-i\alpha_p s) \tag{9}$$

The coefficients are found from minimization of the energy and normalization of the eigenfunctions. The eigenfunctions, shown in Fig.1, are eigenfunctions of parity [20] and parity is conserved during translocation. The eigenvalues are determined by the boundary conditions.

For odd values of p=1,3..., the functions are symetrical:

$u_p(s) = \cos(\alpha_p s)/(\cos \alpha_p L/2) + \cosh \alpha_p s/(\cosh \alpha p L/2)$

with

$(\tan \alpha_p L/2)/(\tanh \alpha_p L/2) = -(\epsilon \alpha_p^2 - \kappa)/(\epsilon \alpha_p^2 + \kappa)$

For even p=2,4.. ,the functions are antisymetrical:

$u_p(s) = \sin(\alpha_p s)/(\sin \alpha_p L/2) + \sinh \alpha_p s/(\sinh \alpha_p L/2)$

with

$(\tan \alpha_p L/2)/(\tanh \alpha_p L/2) = (\epsilon \alpha_p^2 + \kappa)/(\epsilon \alpha_p^2 - \kappa)$

The eigenvalues are well approximated by $\alpha_p = (2p+1)\pi/2L$. For odd parity, an additional eigenvalue is found at $\alpha_p = \pi/L$. This solution disappears for $\kappa = 0$.

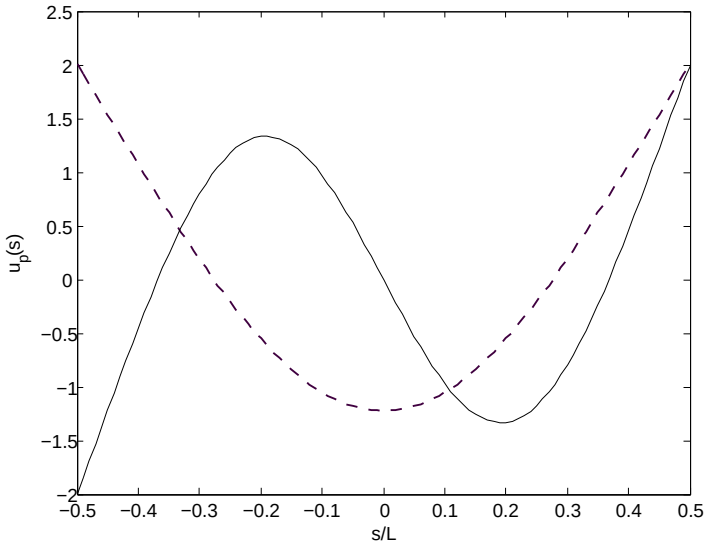

FIG. 1: The eigenfunctions of the bend and stretch elastic chain for p = 1 (dashes) and p = 2 (line)

The equation of motion for the time dependent functions $q_p(t)$ is found from eq.(4). An expansion in the wall anchoring field is used to first order in W:

$$\frac{\partial^2 q_p(t)}{\partial t^2} + \zeta \frac{\partial q_p(t)}{\partial t} + ((\epsilon/m)\alpha_p^4 - (\kappa m)\alpha_p^2 - F_1/m)q_p(t) = B_0(p,t) + B_1(p,t) \qquad (10)$$

The frequency of the polymer mode $p > 0$ is

$$\omega_{1,2}(p) = -\zeta/2 \pm \sqrt{\zeta^2 - 4((\epsilon/m)\alpha_p^4 - (\kappa/m)\alpha_p^2 - F_1/m)}/2 \qquad (11)$$

The solution for $q_p(t)$ for $p > 0$:

$q_p(t) = \frac{1}{\omega_1(p)-\omega_2(p)}[\int dt'(B_0(p,t') + B_1(p,t'))(\exp(\omega_1(p)(t-t')) - \exp(\omega_2(p)(t-t'))) - q_p(0)(\omega_2(p)\exp(\omega_1(p)t) - \omega_1(p)\exp(\omega_2(p)t)) + \frac{\partial q_p(0)}{\partial t}(\exp(\omega_1(p)t) - \exp(\omega_2(p)t))]$

The fluctuating force is $B_0(p,t) = \int dsA(s,t)u_p(s)/mL$ and fulfills

$< B_0(p,t)B_0(p',t) >= 4\frac{kT\zeta}{mN}\delta(t-t')\delta(p,p')$.

An additional force arises from the fluctuations of q_p in the anchoring field: $\frac{3W}{2m}\int dsu_p(s)(\partial z/\partial s)^2/L$ with $< B_1(p,t) >= \frac{3W}{2m}Q_pS_p(t)$. The related order parameter for odd p is $Q_p = \int dsu_p(s)(\frac{\partial u_p}{\partial s})^2/L$. For even p, $Q_p = 0$. The time correlation function $S(p,p',t) =< q_p(t)q_{p'}(t') >$ can be calculated using eq. 10. It is expected that the system becomes stationary after a long time so that the correlation function for $\zeta t >> 1$ is:

$S(p,p',t\to\infty) = S(p) = \frac{kTa}{L}[\epsilon\alpha_p^4 - \kappa\alpha_p^2 - F_1]^{-1}\delta(p,p')$

2.2.2. Case $p = 0$:

A particular solution of the equation is given for p=0. From eq. 4, the solution is $u_0(s)q(t)$ with $\epsilon\frac{\partial^4 u_0}{\partial s^4} - \kappa\frac{\partial^2 u_0}{\partial s^4} = 0$. Due to the boundary conditions $u_0(s) = 1$ and $q_0(t)$ is solution of:

$$\frac{\partial^2 q_0(t)}{\partial t^2} + \zeta \frac{\partial q_0(t)}{\partial t} + W/2m - F_0/m - F_1 q(t)/m = B_0(t) + B_1(t) \qquad (12)$$

The fluctuating force is again composed of two terms. The random white noise for the $p = 0$ mode is $B_0(t) = \int dsA(s,t)/mL$. The fluctuating wall friction force for the $p = 0$ mode is $B_1(t) = \frac{3W}{2m}\int ds(\frac{\partial z}{\partial s})^2/L$. The orientation correlation in the z-direction is given by $\sigma_p = \int ds(\frac{\partial u_p(s)}{\partial s})^2/L$ and the average fluctuating force due to the anchoring field is $< B_1(t) >= \frac{3W}{2m}\sum_{p=1}\sigma_pS_p(t)$. In the following $< B_1(t) >= \frac{3W}{2m}\sigma$ with $\sigma = \sum_p \sigma_pS_p(t)$.

The frequencies are found from the equation of motion (12).

For $F_1 = 0 : \Omega_1 = 0, \Omega_2 = -\zeta$. For $F_1 \neq 0$:

$$\Omega_{1,2} = -\zeta/2 \pm [\sqrt{\zeta^2 + 4F_1/m}]/2 \tag{13}$$

For $F_1 = 0$ the solution for $q_0(t)$ is

$q_0(t) = \frac{1}{\zeta}[\int dt'(F_0/m - W/2m + B_0(t') + B_1(t'))(1 - \exp(\zeta(t' - t))) + q_0(0) + \frac{\partial q_0(0)}{\partial t}(1 - \exp(-\zeta(t)))$

For $F_1 < 0$ the solution for $q_0(t)$ is

$q_0(t) = \frac{1}{\Omega_1 - \Omega_2}[\int dt'(B_0(t') + B_1(t'))(\exp(\Omega_1(t - t')) - \exp(\Omega_2(t - t'))) - q_0(0)(\Omega_2 \exp(\Omega_1 t) - \Omega_1 \exp(\Omega_2 t)) + \frac{\partial q_0(0)}{\partial t}(\exp(\Omega_1 t) - \exp(\Omega_2 t))] - F_0/F_1 + W/2F_1$

The dynamics of the macromolecule can now be discussed.

2.3 The polymer dynamics

The random motion of the elastic chain is superimposed on the orientation by the pore walls and drift caused by the electrostatic forces. The average motion of center of mass is found from $Z_g(t) =< \int dsz(s,t)/L >=< q_0(t) >$. Using the initial conditions $Z_g(t = 0) = Z_g(0); \frac{\partial Z_g(t=0)}{\partial t} = v_0$. the center of mass at time t is located at

$$Z_g(t) = Z_g(0) + v_0(1 - \exp(-\zeta t))/\zeta + (F_0 + W(3\sigma - 1)/2)(\zeta t + \exp(-\zeta t) - 1)/m\zeta^2 \tag{14}$$

for $F_1 = 0$ and for $F_1 \neq 0$:

$Z_g(t) = Z_g(0)\frac{\Omega_1 \exp \Omega_2 t - \Omega_2 \exp \Omega_1 t}{\Omega_1 - \Omega_2} + \frac{v_0(\exp \Omega_1 t - \exp \Omega_2 t)}{\Omega_1 - \Omega_2} + (\frac{\Omega_1 \exp \Omega_2 t - \Omega_2 \exp \Omega_1 t}{\Omega_1 - \Omega_2} - 1)(F_0/F_1 + W(3\sigma - 1)/2F_1)$

As the polymer diffuses through the pore the initial velocity decays and the average monomer velocity $< \int dsv(s) > /L = \frac{\partial Z_g(t)}{\partial t}$ contains a contribution from the pore wall interaction.

A measure of the extension along z is found from the z component of the center to end distance vector: $R_z(t) =< z(L/2,t) - z(0,t) >$. Calculated using eq. (10) and (12), $R_z(t) = 2\sum_{p=1} < q_p(t) >$.

For short times $t\zeta < 1$ the extension is defined by the initial conditions:

$R_z(t) = R_z(0) + t\frac{\partial R_z(0)}{\partial t}$

and at long times $t\zeta >> 1$ R_z reaches a constant value $R_z(\infty)$.

$R_z(\infty) = 3W \sum_{p=1} \frac{S(p)Q_p}{\epsilon(\alpha_p)^4 - \kappa(\alpha_p)^2 - F_1}$

3. DISCUSSION

3.1 Effect of chain elasticity

The dynamics of flexible stretch elastic chains are well known: the modes are given by a Fourier series with appropriate boundary conditions: $u_p(s) = \cos(p\pi s/L)$. The equilibrium average $<< .. >>$ of the mode coordinates determines the stretch elastic coefficent of the p mode from equipartition [13]; the end to end distance is $<< R^2 >>= La$ and $\kappa = kT/a$.

Bend elasticity adds the exponential functions to describe the polymer modes and a typical conformation, given in eq. (9), is shown in Fig.1. Here the zero order "rigid rod" mode proportional to s is an unphysical solution of zero bend energy and maximum stretch energy and is not retained [17]. For semi rigid chains the stretch elastic coefficient is set to zero and the chain avoids bend deformations by increasing the effective size of the polymer chain. In the wormlike chain model only those chain conformations which fulfill the condition of constant length or $\left|\frac{d\vec{r}}{ds}\right| = 1$ are considered in the calculation of the probability distribution [15]. The bend elastic coefficent is then simply related to the correlation length b of the chain orientation: $\epsilon = kTba$. In the rigid chain limit, $L/b < 1$;the persistence length b is large and the end to end distance of the bend chain is calculated as $<< R^2 >> /L^2 \approx 1$. In DNA the persistence length is given as b/a = 80 and in the Molecular Dynamics simulation to which results will be compared b/L=4 [11]. The bend elastic constant also changes the time evolution of the polymer modes with a strong dependence of the frequency in L^4 and not L^2 as for stretch polymers.

The intermediate case of finite stretch and bend has been investigated [5–7, 17–20] and by use of the appropriate eigenfunctions chain dynamics were studied in the presence of external fields. Finite stretch combined with bend modifies the frequencies and decay times of the polymer modes. As in stretch chains, the bend elastic coefficent for the p mode is

determined from the equilibrium distribution of $<< q_p^2 >>$ and the equilibrium end to end distance is found for $t \to \infty$:

$<< R^2 >> = (3kTa/L) \sum_p [\epsilon \alpha_p^4 - \kappa \alpha_p^2]^{-1}$.

For weak bend, $\epsilon/\kappa << 1$, the end to end distance of stretch elastic chains is recovered. In the case of rigid chains with strong bend, $\epsilon \pi^2/(4\kappa L^2) >> 1$, the contributions from the bend and stretch modes compensate [19, 20] and the end to end distance is determined mainly by the antisymetric mode $\alpha_p L = \pi$. The bend elastic coefficient $\epsilon = 12kT(32aL/\pi^4)$ is then found to lie close to the value of DNA in the simulation. Equilibrium properties of bend elastic chains in the stationary limit of the normal mode analysis will not be equivalent to the same quantities calculated in the wormlike chain model since an average over conformations with a different set of restrictions is performed. The two approaches will be equal only if the sampling in both cases is sufficiently thorough to capture typical behaviour. The parameter σ is a measure of the deviation from the geometric wormlike chain model.

3.2 Effect of friction

The effective friction coefficient determines the decay times for polymer dynamics on entering and leaving the pore. The value can be estimated from the diffusion constant D of the single chain of degree of polymerization L/a in the relevant solvent. Neglect of the hydrodynamic interaction is justified for sufficiently wide pores. From a reasonable value of diffusion constant $D = 10^{-6} cm^2 s^{-1}$ and monomer mass $m = 10^{-21} g$ the monomer friction coefficient is found to be of the order of $10^{13} s^{-1}$.

3.3 Effect of electric field

The electric field inside the pore is given by eq. (3) and plotted in Fig.2.

The similarity with the field obtained by MD simulation [11] for a synthetic nanopore is visible. A small variation of the gradient of the electric field in z justifies the expansion at the pore center used in the calculation for pores with $R/H > 1/2$ and shown in Figure 3.

In the simulation R/H = 0.2 and variation of the electric field gradient is large as shown

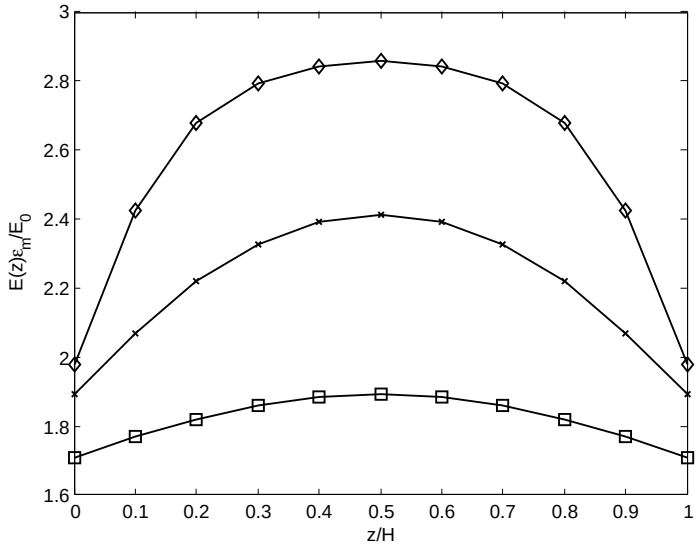

FIG. 2: Induced pore electric field E(z)relative to the applied electric field in the solvent of dielectric constant ϵ_m as a function of distance z on the pore axis for different pore geometry R/H = 0.2 (diamonds), 0.5 (crosses), 1 (squares). The pore dimensions are R, radius; H, height.

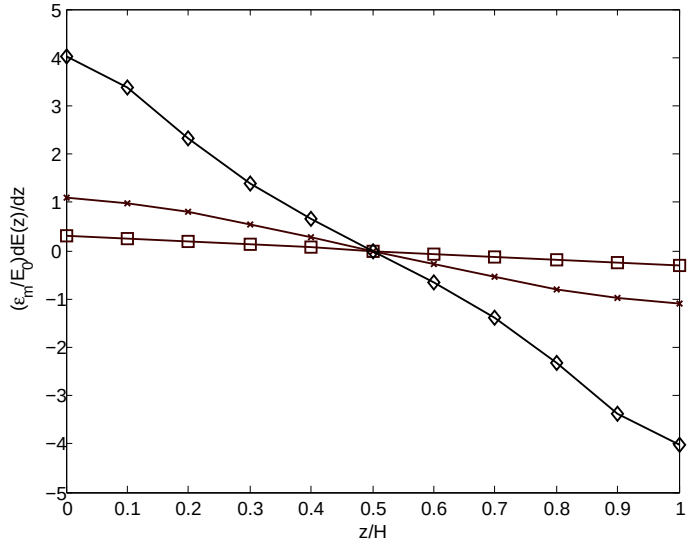

FIG. 3: The gradient $dE(z)/dz$ of the induced pore electric field E(z)relative to the applied electric field in the solvent of dielectric constant ϵ_m as a function of distance z on the pore axis for different pore geometry R/H = 0.2 (diamonds), 0.5 (crosses), 1 (squares). The pore dimensions are R, radius; H, height.

in Fig.3. In order to accelerate the translocation from ms to ns, the applied electric field of the simulation is 1.4V; typically in experiments a field of the order of mV is applied.[11] To compare results, a value of $F_0 = 5 \cdot 10^{-5}$gcms^{-2} is obtained from the simulation for H = 5nm , R = 1nm. Outside the pore chain translation is due to acceleration by the uniform applied field and the chain arrives at the pore entrance with a velocity $v_0 = eE_0/\epsilon m\zeta = 1cms^{-1}$. The motion of the center of mass of the chain inside the pore is plotted in Fig. 4. The chain motion is initially linear in time and after a time ζ^{-1} the chain motion is driven by the internal pore field with a velocity $v_\infty = F_0/m\zeta + W(3\sigma - 1)/2m\zeta$. The electric force dominates the translation of the chain through the pore and in particular the field gradient over the uniform field due to the screening of the polyelectrolyte by the free ions. The translocation time τ is measured by the time for the center of mass to exit the pore with $Z_g(\tau) = H + L/2$. From the simulation, the velocity $v_\infty = 5 \cdot 10^3 cms^{-1}$ and $\tau = m\zeta(H + L/2)/F_0$. The translocation time is inversely proportional to the applied field and proportional to the polymer length as found in experiment. Outside the pore the velocity of the polymer center of mass returns to the value v_0 within $\zeta^(- 1)$.

Experiments have been made in the presence of an optical trap placed at the end of the pore [1]. A field is created proportional to the distance of the chain to the pore end as given by the term in F_1. The chain motion shown in Fig.4 is initially linear in time but stops at a finite stationary value after a time t_c which is inversely proportional to the field constant F_1. If the chain exits the pore before this time is reached then the translocation time is calculated from the initial velocity as $\tau = m\zeta(H + L/2)/eE_0 = 2500ns$. Then as before the translocation time is inversely proportional to the applied field and proportional to the polymer length. The optical trap affects the chain velocity and the time needed to block the polymer within the pore is smaller the larger the strength of the trap.

3.4 Effect of the pore walls

The interaction with the pore walls accelerates the translation of the polymer chain and contributes to the motion of the center of mass. For strong bend and weak stretch, the order parameter is calculated from (10):

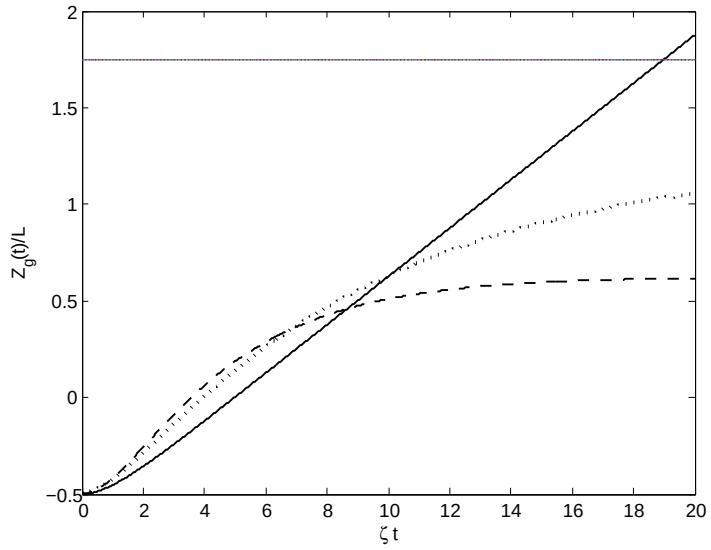

FIG. 4: Motion of the center of mass Z_g/L of the polymer of length L as a function of time ζt and for different values of stiffnes of the optical trap: $F_1/m\zeta^2 = 0$ (line), -0.1(dots), -0.2(dashes).The straight upper line corresponds to the translocation time.

$\sigma = \sum_{peven}[\alpha_p^2 + 3\alpha_p/L]S(p) + \sum_{podd}[\alpha_p^2 + 4\alpha_p/L]S(p) + [(\pi/L)^2 + 3\pi/(L^2)]$

The contribution from the odd parity mode with $\alpha_p = \pi/L$ again dominates. For the parameters of the DNA simulation, σ lies close to two and for $WL/kT = 50$ the velocity term from the pore wall friction is an order of magnitude smaller than that of the induced electric field in the pore.

The wall friction affects the polymer conformation and the extension of the chain increases in the z-direction. The order parameter is calculated as $Q_p = 2\alpha_p \frac{1+cos\alpha_p L}{5Lcosh\alpha_p L/2}$.

The evolution with time of the projection of the center to end vector along the pore axis is plotted in Fig.5.

The extension initially increases slowly with time; the rapidly damped vibrations due to the polymer modes are not shown. The frequencies of the vibrating polymer modes for large p are $\Omega_p^2 = (\epsilon/m)(\alpha_p)^4 = (2p+1)^2 \times 10^8 s^{-1}$ for the parameters of the DNA simulation. After a time of the order of $\omega_1(p=1)^{-1} \approx \zeta^{-1}$, a fixed finite value of the projection is reached which depends on the effective wall interaction. After exiting the pore the extension decays to the value of free chains $R_z = 0$ within a time ζ^{-1}. The maximum average extension of the polymer on exiting the pore is about 0.2 of the chain length for a friction force $W/kT = 50/H$. This corresponds to an average value of the center to end vector projected onto the pore axis; local order may be much greater. For large pores it was shown in a molecular dynamics simulation [10] that ordering of the polymer is large mainly when the chain is located a few nanometers from the pore walls. The extension consists here of orientation of the monomers as well as a change of monomer length; in the calculation, stretch elasticity of the polymer was not considered nor any constraint set for constant total length of the chain. A strong dependence on the polymer length is obtained; if the chain length is doubled, the extension is increased by a factor 2^5 and $R_z/L \to 1$.

In the presence of the optical trap, the stationary chain extension is reached in a time $t_c \approx \zeta m/(-F_1)$ inversely proportional to the field constant. The extension is blocked at a small value which is also inversely proportional to the field strength. For $F_1/m\zeta^2 = -0.1$ the maximum extension is $R_z/L = 0.1$ and the time needed to block the chain and reach maximum extension is $t_c = 10\zeta^{-1}$, which is smaller than the translocation time τ as seen in Figure 4.

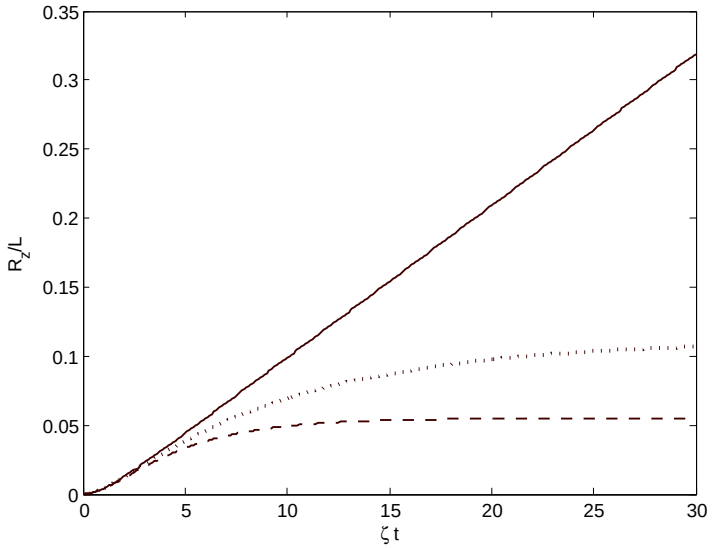

FIG. 5: Projection R_z/L of the center to end distance of the polymer of length L (L/a=20) as a function of time ζt and for different values of stiffnes of the optical trap: $F_1/m\zeta^2 = 0$ (line), -0.1 (dots), - 0.2 (dashes) in a wall potential $W/(mL\zeta^2) = 10^{-4}$.

4. CONCLUSIONS

In this paper we have examined the motion of a semi rigid polymer in a nanopore.The improvements of the present model go beyond the use of a flexible model and simply increasing the effective monomer length(or decreasing the stretch elasticity) to a value consistent with the persistence length. In contrast to flexible polymers described by a stretch elasticity, bend elastic chains can be oriented in an external field, here the anchoring field created by the pore atoms. For anchoring of the polymer parallel to the pore axis the walls of the pore must not be smooth. Surface roughness is consistent with the complex potential profiles of synthetic and natural pores where internal sites, trapped charges and complex structure occur. For example, silicon dioxide surfaces can have a negative charge density possibly neutralized by counter ion condensation. The transition time for the polymer to pass through the nanopore is determined mainly by the applied pore field within the pore. The drift through the pore is superimposed on random damped motion of the monomers and a continuous change of conformation. The electric field gradient inside the pore couples to the dipoles of the chain and decreases the time required for translocation inside the pore. Application of a force proportional to the distance of the exit to the end of the pore such as an optical trap slows down the motion, and reduces the chain response to the wall potential and the extension along the pore axis. This technique in combination with more complex pore geometry may prove useful in future nanopore studies. A vast amount of experimental, theoretical and simulation work exists for DNA translocation. The two approaches of phenomenological modeling (as used here) and molecular dynamics are complementary. On the one hand the phenomenological description of polymer dynamics makes it possible to study dependence on important parameters of the system such as pore length, geometry, and applied field. But for more detailed knowledge such as the effect of atomistic structure a description based on molecular dynamics cannot be avoided. DNA is a well known semi rigid polymer and Langevin dynamics based on bend elasticity should provide a good qualitative picture and help to determine optimal conditions for a given experiment.

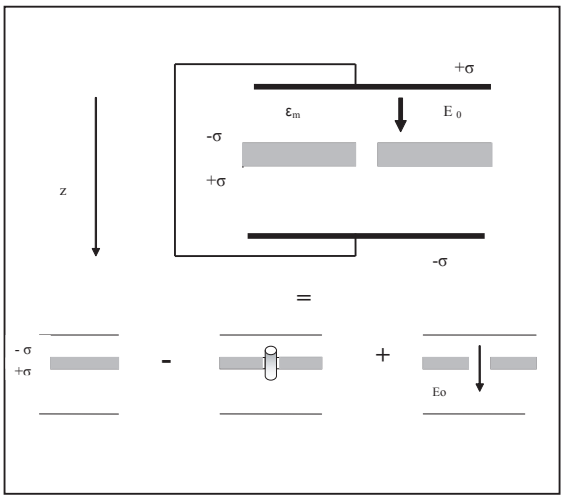

FIG. 6: The components of the electric field within the pore

APPENDIX I

The set up is given in Figure 6. The field is approximated by the field induced by surface charges on the upper and lower plates superimposed on the dielectric cavity formed by the pore.

First the membrane is replaced by charged plates at spacing H with induced charge $\mp\sigma$ on the upper and lower surfaces. The cylinder of radius R, charged on upper and lower surfaces, is removed to form the pore and then replaced by the applied electric field E_0 in the dielectric medium of dielectric constant ϵ_m.

* Electronic address: tenbosch@unice.fr

[1] M. Zwolak and M. DiVentra, Rev. Modern Physics **80**, 141 (2008).

[2] J. Lagerqvist, M. Zwolak, and M. DiVentra, Biophysics **93**, 2384 (2007).

[3] K. Luo, I. Huopaniemi, T. AlaNissala, and S. Ying, Journal of Chemical Physics **124**, 114704 (2006).

[4] C. Forrey and M. Muthukumar, Journal of Chemical Physics **127**, 05102 (2007).

[5] J. Wang and H. Gao, Journal of Chemical Physics **123**, 084906 (2005).

[6] J. Wang and H. Gao, Journal of Materials Science **42**, 8838 (2007).

[7] L.X.Zhang, A. Xia, and D. Zhao, European Polymer Journal **37**, 1277 (2001).

[8] Y. Chen, M. Graham, J. DePablo, C. Randell, M. Gupta, and P. Doyle, Physical Review E **70**, 060901 (2004).

[9] K. Luo, T. AlaNissala, S. Ying, and A. Bhattacharya, Physical Review Letters **99**, 148102 (2007).

[10] F. Zhang, Journal of Chemical Physics **111**, 9082 (1999).

[11] J. Heng, A. Aksimentiev, C. Ho, P. Marks, Y. Grinkova, S. Sligar, K. Schulten, and G. Timp, Biophysical Journal **90**, 1098 (2006).

[12] M. Gracheva, A. Xiong, A. Aksimentiev, K. Schulten, G. Timp, and J. Leburton, Nanotechnology **17**, 622 (2006).

[13] M. Doi and S. Edwards, *The Theory of Polymer Dynamics* (Oxford Science, 1986).

[14] M. Bawendi and K. Freed, Journal of Chemical Physics **83**, 2491 (1985).

[15] A. ten Bosch, Makromol. Chem. ;Theory, Simulations **3**, 851 (1993).

[16] P. Benetatos and F. E, Physical Review E **70**, 051806 (2004).

[17] R. Harris and J. Hearst, Journal of Chemical Physics **44**, 2595 (1965).

[18] N. Saito, K. Takahasi, and Y. Yunoki, Journal of Physical Society of Japan **22**, 219 (1967).

[19] K. Soda, Journal of Physical Society of Japan **35**, 866 (1973).

[20] S. Aragon and R. Pecora, Macromolecules **18**, 1868 (1985).

[21] A. Maggs, Physical Review Letters **85**, 5472 (2000).

[22] B. Jerome, Rep. Prog. Phys. **54**, 393 (1991).

[23] A. ten Bosch, Physical Review E **63**, 0 (2001).

[24] L. Klushin and F. A. M. Leermakers, Physical Review E **66**, 036114 (2002).

[25] P. Wiggins, T. van der Heijden, F. Moreno-Herrero, R. Phillips, J. Widom, C. Dekker, and P. Nelson, Nature **1**, 87 (2006).

[26] R. Jendrejack, E. Dimalanta, D. Schwartz, M. Graham, and J. DePablo, Phys. Rev. Letters **91**, 038102 (2005).

[27] J. Dzubiella and J. Hansen, Journal of Chemical Physics **122**, 234706 (2005).

[28] E. Durand, *Electrostatique I* (Masson Paris, 1964).

[29] Y. Rabin and M. Tanaka, Physical Review Letters **94**, 148103 (2005).

[30] S. Ghosal, Physical Review E **74**, 04901 (2005).

[31] M. Fixman, Journal of Chemical Physics **76**, 6346 (1982).

[32] T. Barrett, Physics Letters **94A**, 59 (1983).

[33] J. Rayleigh, *The Theory of Sound* (Dover Publications, 1945).